Structural Biology of the Major Facilitator Superfamily Transporters

Nieng Yan

State Key Laboratory of Bio-membrane and Membrane Biotechnology, Center for Structural Biology, School of Medicine, Tsinghua-Peking Joint Center for Life Sciences, Tsinghua University, Beijing 100084, China; email: nyan@tsinghua.edu.cn

Annu. Rev. Biophys. 2015. 44:257–83

The *Annual Review of Biophysics* is online at biophys.annualreviews.org

This article's doi: 10.1146/annurev-biophys-060414-033901

Keywords

major facilitator superfamily, MFS, alternating access, membrane transport, GLUT1

Abstract

The ancient and ubiquitous major facilitator superfamily (MFS) represents the largest secondary transporter family and plays a crucial role in a multitude of physiological processes. MFS proteins transport a broad spectrum of ions and solutes across membranes via facilitated diffusion, symport, or antiport. In recent years, remarkable advances in understanding the structural biology of the MFS transporters have been made. This article reviews the history, classification, and general features of the MFS proteins; summarizes recent structural progress with a focus on the sugar porter family transporters exemplified by GLUT1; and discusses the molecular mechanisms of substrate binding, alternating access, and cotransport coupling.

Contents

INTRODUCTION

More than 800 genes in the human genome are thought to encode membrane transport proteins (37). These proteins have evolved to shepherd a wide variety of essential molecules, ranging from protons to folded proteins, as they move through the hydrophobic lipid bilayer. Transport proteins have been identified for even the small neutral molecules water and glycerol, which had been thought to traverse membrane merely via free diffusion (2). The presence of highly specific and diverse transport proteins provides the first layer of sophisticated regulation at the boundary between an organism and its environment. Transport proteins play a pivotal role in cellular growth, homeostasis, metabolism, and signal transduction.

Transport proteins comprise channels and transporters. Channel proteins are open to both sides of the membrane simultaneously when in a conducting state, and therefore they mediate only the diffusion of substrates down their electrochemical gradients. In contrast, transporters are capable of catalyzing the transmembrane movement of specific substrates uphill against their concentration gradients. To observe thermodynamic laws, a transporter must harness other forms of energy to drive the uphill translocation of specific substrates. Transporters can be classified into three types depending on their energy source: primary active transporters, secondary active transporters, and facilitators. Primary active transporters are powered by photons or by energy released from chemical reactions such as ATP hydrolysis. Secondary active transporters exploit the electrochemical potentials of a cotransporting ion or solute, such as a transmembrane proton or sodium gradient. To achieve energy coupling, a transporter must possess at least two gates that open alternately, never simultaneously (27, 93). Facilitators, also called uniporters, catalyze

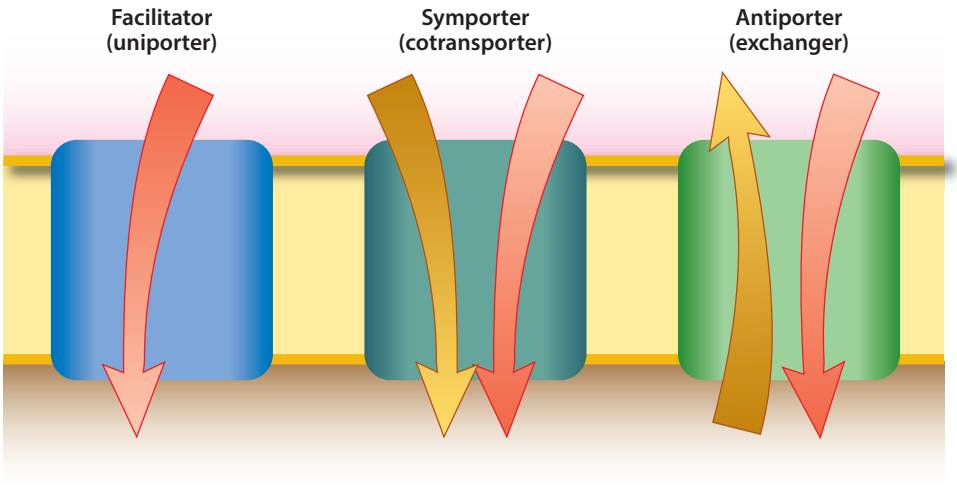

Figure 1

Schematic illustration of the three types of secondary active transporters. Facilitators catalyze substrate diffusion across the membrane down its concentration gradient. Symporters or antiporters use the energy released from the downhill translocation of one substrate to drive the uphill translocation of another substrate either in the same direction (symporters) or in the opposite direction (antiporters). The color gradients of the arrows indicate the transmembrane electrochemical gradients of the substrates.

diffusion of the substrates down their electrochemical gradients. These transporters are sometimes considered a subtype of secondary transporters that lacks cotransport coupling. In this article, the term "secondary transporters" refers to both secondary active transporters and facilitators.

The major facilitator superfamily (MFS) represents the largest among all groups of secondary transporters (20, 44, 90). This article reviews the research history, classification, and general structural features of these proteins, with a focus on recent advances in their structural biology.

THE MAJOR FACILITATOR SUPERFAMILY

The MFS is an ancient and ubiquitous transporter superfamily consisting of more than 15,000 sequenced members, and this number is growing rapidly with the continuing emergence of genome sequences (20, 44). Members of the MFS have an extraordinarily broad spectrum of substrates, including inorganic and organic ions, nucleosides, amino acids, short peptides, and lipids. MFS members comprise facilitators, symporters, and antiporters, which move substrates across membranes via facilitated diffusion, cotransport, or exchange, respectively (**Figure 1**). Owing to their fundamental significance in physiology, pathophysiology, and drug development, the MFS transporters, exemplified by the human glucose transporters GLUT1, GLUT2, GLUT3, and GLUT4 and by the *Escherichia coli* lactose permease LacY, have been the most rigorously investigated transporters with a long history.

The Early History of Major Facilitator Superfamily Protein Research

Studies of glucose permeation, the Na^+:K^+ pump (95), and action potentials (43) represent the early history of research into transporters, ion pumps, and ion channels, respectively. The earliest examination of glucose transport through biomembranes occurred nearly a century ago. In 1919, Edge reported in his thesis that the rate of glucose permeation through the human red blood cell

membrane was affected by glucose concentration, an observation that was further confirmed by more systematic and quantitative examinations in 1930s and 1940s (4, 108). In 1948, LeFevre (64) provided experimental evidence supporting an active transport mechanism for glucose uptake into human red blood cells. He postulated a "carrier" concept without details as to molecular mechanism. In the early 1950s, Widdas (106, 107) elaborated on the carrier transfer hypothesis, extending it to account for the observed kinetics of placental glucose transfer. In the late 1970s, a liposome-based glucose uptake assay was reconstituted with partially purified proteins from erythrocytes (56, 57). The glucose transporter from red blood cells was then named GLUT1, and its amino acid sequence and 12–transmembrane segment (TM) topology were deduced by Lodish and colleagues in 1985 (73). Subsequently, three additional tissue-specific glucose transporters, GLUT2, GLUT3, and GLUT4, were cloned (5, 25, 26, 50, 102). The focus of GLUT research was then shifted toward identification and characterization of their disease-related variants and toward their mechanisms of regulation, structural characterization, and potential as drug targets (74).

LacY, one of three genes in the *Lac* operon (48, 49), was the first for which a gene product was shown to be associated with a specific transport activity (17, 23, 24). The transport function of LacY was extensively studied at a genetic level prior to 1980 (94). In 1980, Kaback, who had successfully prepared membrane vesicles derived from *E. coli* in the 1960s (55), demonstrated the proton gradient–dependent transport activities of LacY in isolated membrane vesicles (89). Since then, the Kaback group (30, 54) has conducted systematic investigations of LacY using a combination of biochemical, biophysical, and structural biology approaches.

In addition to GLUTs and LacY, dozens of MFS transporters have been identified that actively transport specific solutes, ions, and drugs in a wide variety of species, including bacteria, fungi, plants, and animals (36). The term "major facilitator superfamily" was coined in 1993 in an effort to phylogenetically classify these sequenced solute permeases and drug-resistance proteins (71). At that time, fewer than 60 proteins, comprising five clusters, were identified as belonging to the MFS. Since then, the number of sequenced and annotated MFS proteins has expanded rapidly (90).

Classification

Three major nomenclature and classification systems have been proposed for transporters. The Pfam protein families database is a comprehensive database of sequenced protein domains from all organisms (20), in which related protein families are grouped into clans. As of September 2014, the MFS clan (CL0015) consists of 25 families and 249,360 sequenced domains (**http://pfam.xfam.org/clan/MFS**) (**Table 1**).

The HUGO Gene Nomenclature Committee (HGNC) uses the solute carrier (SLC) system to classify human genes that encode membrane transport proteins, excluding channel proteins, ABC transporters, and ion pumps (37). In total, 395 genes in the human genome have been assigned to 52 SLC families (**http://slc.bioparadigms.org/**). Among these, 14 SLC families comprising 102 genes belong to the MFS (**Table 1**) (3).

A third classification system is presented by the Transport Classification Database (TCDB, **http://www.tcdb.org/**), which classifies representative transporters from all organisms on the basis of transport mechanism (two criteria), phylogenetic relations (two criteria), and substrates (one criterion), and which has a superfamily > family > subfamily hierarchy. In the TCDB, 8 of over 600 families, consisting of 864 annotated proteins, belong to the major facilitator superfamily (a superfamily that contains the MFS), and the MFS family (2.A.1) is further divided into 82 subfamilies (**Table 1**) (90).

Notably, structural biology has provided important insights into the understanding of the evolution and classification of membrane transporters. Proteins having no sequence similarity may

Table 1 Major facilitator superfamily (MFS) members and subfamilies in the Pfam, SLC, and TCDB databases

Members of the MFS clan (CL0015) in the Pfam database (249,360 domains)		
Acatn		
ATG22		
BT1		
CLN3		
DUF1228		
DUF791		
Folate carrier		
FPN1		
FTR1		
LacY Symp		
MFS 1		
MFS 1-like		
MFS 2		
MFS 3		
MFS *Mycoplasma*		
Nodulin-like		
Nuc H symport		
Nucleoside tran		
OATP		
PTR2		
PUCC		
Sugar tr		
TLC		
TRI12		
UNC-93		
Genomic Transport Database solute carrier series (SLC) families belonging to the MFS (102 proteins)		
ID	*Family description*	*Number of identified proteins*
SLC2	Facilitative glucose transporters	14
SLC15	Proton oligopeptide cotransporter	4
SLC16	Monocarboxylate transporter	14
SLC17	Vesicular glutamate transporter	9
SLC18	Vesicular amine transporter	4
SLC19	Folate/thiamine transporter	3
SLC21/SLCO	Organic anion transporter	12
SLC22	Organic cation/anion/zwitterion transporter	23
SLC29	Facilitative nucleoside transporter	4
SLC33	Acetyl-CoA transporter	1
SLC37	Sugar-phosphate/phosphate exchanger	4
SLC43	Sodium-independent, system-L like amino acid transporter	3
SLC45	Putative sugar transporter	4
SLC46	Folate transporter	3

(*Continued*)

Table 1 (*Continued*)

Transport Classification Database (TCDB) families belonging to the MFS (864 proteins)		
ID	*Family description*	*Number of proteins*
2.A.1	Major facilitator superfamily (MFS)	728
2.A.2	Glycoside-pentoside-hexuronide:cation symporter (GPH) family	37
2.A.12	ATP:ADP antiporter (AAA) family	20
2.A.17	Proton-dependent oligopeptide transporter (POT/PTR) family	40
2.A.48	Reduced folate carrier (RFC) family	6
2.A.60	Organo anion transporter (OAT) family	23
2.A.71	Folate-biopterin transporter (FBT) family	8
9.B.111	6TMS Lysyl tRNA synthetase (LysS) family	2

exhibit identical structural folds. For example, the structure of the formate channel FocA reveals an unexpected aquaporin fold (75, 105), and, consequently, the formate–nitrite transporter (FNT) family is now included in the major intrinsic protein (MIP) superfamily in the TCDB. Rapid progress in the structural identification of proteins with a leucine transporter (LeuT) fold has led to the reassignment of 11 families into the amino acid–polyamine-organocation (APC) superfamily (28, 111, 113). Thus, more families, for which structural information remains unknown at present, may eventually be included in the MFS.

These parallel classification and nomenclature systems have brought a certain degree of complexity and confusion. Each of the three systems has a distinct emphasis, however, so it cannot replace the others. The SLC system focuses on human transporters, whereas Pfam analyzes millions of sequences and classifies them based on domains. Effort has been made to correlate the Pfam and SLC systems (44). In this review, I rely on primarily the TCDB system when discussing representative proteins.

General Transport Mechanism

Our understanding of the general transport mechanism has been advanced as a result of decades of multidisciplinary studies. The solute carrier mechanism proposed by Widdas (107) has been gradually replaced by a more general alternating-access mechanism (51). The carrier mechanism suggests that transport of the solute requires a carrier (the transporter) that loads the substrate on one side of the lipid bilayer, swims across the membrane, and releases the cargo on the other side (107). The alternating-access mechanism, in contrast, predicts that to complete a transport cycle, the transporter must switch between at least two conformations, an outward-facing conformation and an inward-facing one, in order to allow alternating access to the substrate binding site from either side of the membrane (**Figure 2**).

A serious challenge to the carrier mechanism is the energy barrier involved in the transmembrane displacement of a protein that presumably has an exposed hydrophilic surface. Although the alternating-access mechanism has become a prevailing one in the transporter field, however, recent structural studies have provided support for the "carrier" mechanism for several specific types of transporters, such as the bacterial aspartate transporter Glt_{Ph} (88), the Na^+:H^+ antiporters NhaA and NapA (63), the bile acid transporter ASBT (123), and the primary active energy-coupling factor (ECF) transporter (104, 112, 119). In these transporters, one domain, either the oligomerization domain, as in Glt_{Ph}, NhaA, NapA, and ASBT, or the transport subunit, as in the ECF transporters, provides the framework needed to support the movement of the substrate binding site across the membrane via a rigid-body rotation of the substrate binding

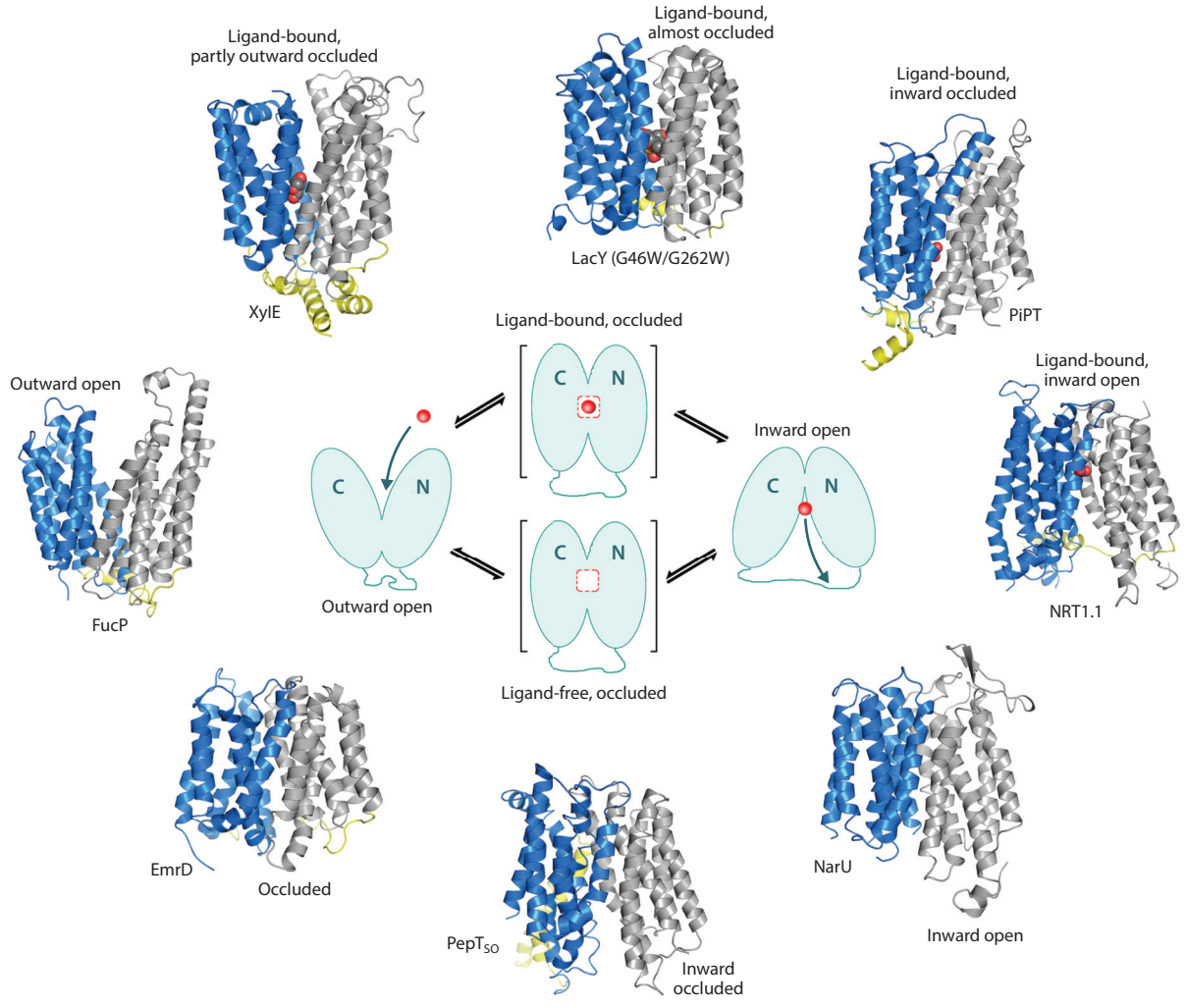

Figure 2

Distinct conformations of major facilitator superfamily (MFS) transporters. The representative structures for MFS transporters exhibit distinct conformations in a predicted alternating-access cycle. The N and C domains are colored in silver and blue, respectively. The bound ligands in XylE, LacY, PiPT, and NRT1.1 are shown as gray spheres. The PDB IDs for these structures are as follows: 3O7Q for FucP, 4GBY for XylE, 4OAA for LacY, 4J05 for PiPT, 4CL5 for NRT1.1, 4IU9 for NarU, 2XUT for $PepT_{So}$, and 2GFP for EmrD. An inventory for these structures can be found in **Table 2**. All structure figures were prepared with PyMol (13). In all side views in this article, the transporters are positioned with the cytoplasmic side at the bottom.

domain (93). This refined carrier mechanism, now referred to as the "elevator mechanism," can still be regarded as a specific form of alternating access. Thus, alternating access represents a general mechanism that can be applied to all known transporters (93, 115).

Physiology, Disease, and Pharmaceutical Perspectives

The MFS transporters have been a major focus of investigation not only because of their abundance, but also, and more importantly, because of their physiological and pathophysiological

significance. As reflected in their names (**Table 1**), the MFS transporters are responsible for nutrient uptake, metabolite extrusion, and multidrug resistance. In essence, these proteins play a pivotal role in growth, metabolism, and homeostasis at cellular level in all organisms, and they are involved in a multitude of physiological processes such as development, neurotransmission, and signaling. Aberrant functions of MFS proteins have been associated with a plethora of debilitating diseases, such as cancer, gout, schizophrenia, epileptic seizure, amyotrophic lateral sclerosis (ALS), and Alzheimer's disease (18, 85, 87). In addition to being drug targets, the MFS transporters can also be employed for specific drug delivery (85).

A recent special issue of *Molecular Aspects of Medicine* was committed to providing a comprehensive review of the current understanding of SLC transporters from physiological, disease, and pharmaceutical perspectives (37). The following MFS families were covered in this issue: the SLC2 GLUT sugar porters (74); the SLC15 proton-coupled oligopeptide transporters (96); the SLC16 monocarboxylate transporters (34); the SLC17 organic anion transporters (87); the SLC18 vesicular neurotransmitter transporters (62); the SLC19 and SLC46 folate transporters (120); the SLC21/SLCO organic anion transporters (33); the SLC22 transporters of organic cations, anions, and zwitterions (58); the SLC29 facilitative nucleoside transporters (118); the SLC33 acetyl-CoA transporters (41); the SLC37 phosphate-linked sugar phosphate antiporters (9); the SLC43 facilitator system L–amino acid transporters (6); and the SLC45 putative sugar transporters (103). The relevance of the MFS transporters to cancer, exemplified by GLUT1, GLUT3, GLUT4, MCT1, MCT4, OCT1, OCT2, and OAT10, was also examined (18). As the expression levels of these transporters change in different types of cancer, activating or inhibiting them may serve as a principle for the development of anticancer drugs. Potential drug-targeting solute carriers, including the SLC2, SLC18, and SLC22 families, have also been studied (85).

The reviews listed above focus on SLC families, which are human transporters. The MFS transporters involved in the multidrug resistance in bacteria and fungi also have the potential for use in the development of new drugs against pathogenic microorganisms. Multidrug resistance and potential uses of MFS transporters from bacteria and fungi have been covered in recent reviews (10, 16).

STRUCTURAL BIOLOGY OF THE MAJOR FACILITATOR SUPERFAMILY TRANSPORTERS

Overview

Before the resolution of any crystal structure, comprehensive biochemical and biophysical approaches were combined to deduce structural information about MFS transporters (45, 53, 101). Electron crystallography was used to examine the structure of a bacterial oxalate:formate antiporter OxlT (40, 42). Despite the relatively low resolution (6.5 Å), the 12 TMs were correctly positioned in the projection. A breakthrough was finally achieved in 2003, when the first crystal structures of two MFS transporters, LacY (1) and the glycerol-3-phosphate transporter, GlpT (46), were reported simultaneously. Despite this inspiring start to the structural investigation of MFS transporters, the determination of new MFS structures proceeded more slowly, with the structure of the multidrug resistance protein EmrD in 2006 (117) and that of the L-fucose:proton symporter FucP in 2009 (11).

A structure boom for the MFS proteins finally arrived during the second decade of the 21st century. As many as 40 structures of 18 unique MFS proteins belonging to 9 MFS families have been deposited in the Protein Data Bank (PDB) as of September 15, 2014 (**Table 2**) (1, 11, 14, 15, 19, 31, 46, 47, 52, 77, 82–84, 97, 99, 100, 110, 114, 117, 121, 122). Although most of

Table 2 Structures, functions, and organisms for which structures of major facilitator superfamily (MFS) proteins have been resolved*

Protein	Function	MFS subfamily and TCDB ID	Organism	PDB ID(s)	Resolution limit (Å)	Year of the first structure	Conformation(s)
GLUT1	D-Glucose facilitator	Sugar porter (SP) 2.A.1.1.28	***Homo sapiens***	4PYP	3.1	2014	Inward open
XylE	D-Xylose:H^+ symporter	SP 2.A.1.1.3	*Escherichia coli*	4GBY, 4GBZ, 4GC0, 4JA3, 4JA4, 4QIQ	2.6	2012	1. Ligand-bound, partly occluded, outward-facing 2. Inward open 3. Partly occluded, inward-facing
GlcP	D-Gluose:H^+ symporter	SP 2.A.1.1.42	*Staphylococcus epidermidis*	4LDS	3.2	2013	Inward open
LacY	Lactose:H^+ symporter	Oligosaccaride:H^+ symporter (OHS) 2.A.1.5.1	*Escherichia coli*	1PV7, 2CFP, 2CFQ, 2V8N, 2Y5Y, 4OAA	2.95	**2003**	1. Inward open 2. Ligand-bound, occluded
FucP	L-Fucose:H^+ symporter	Fucose:H^+ symporter (FHS) 2.A.1.7.1	*Escherichia coli*	3O7Q, 3O7P	3.1	2009	Outward open
PiPT	Phosphate:H^+ symporter	Phosphate:H^+ symporter (PHS) 2.A.1.9.10	*Piriformospora indica*	4J05	2.9	2013	Ligand-bound, inward-facing, occluded
GlpT	Glycerol-3-phosphate:Pi antiporter	Organophosphate:Pi antiporter (OPA) 2.A.1.4.3	*Escherichia coli*	1P24	3.3	**2003**	Inward open
NarU	Nitrate:nitrite antiporter	Nitrate/Nitrite Porter (NNP) 2.A.1.8.10	*Escherichia coli*	4IU8, 4IU9	3	2013	1. Inward-facing, occluded 2. Partially inward open
NarK	Nitrate:nitrite antiporter	NNP: 2.A.1.8.1	*Escherichia coli*	4JR9, 4JRE	2.6	2013	1. Apo inward open; 2. Inward open with nitrite
EmrD	Drug:H^+ transproter	Drug:H^+ antiporter-1 (DHA1) 2.A.1.2.9	*Escherichia coli*	2GFP	3.5	2006	Occluded
YajR	Drug:H^+ symporter	DHA1: 2.A.1.2.60	*Escherichia coli*	3WDO	3.15	2013	Outward open

(*Continued*)

Table 2 (*Continued*)

Protein	Function	MFS subfamily and TCDB ID	Organism	PDB ID(s)	Resolution limit (Å)	Year of the first structure	Conformation(s)
MelB	Melibiose:sodium (or lithium or H^+) symporter	Glycoside-pentoside-hexuronide: cation symporter (GPH) 2.A.2.1.1	*Salmonella typhimurium*	4M64	3.4	2014	1. Outward partly occluded 2. Outward inactive
$PepT_{So}$	Peptide:H^+ symporter	Proton-dependent oligopeptide transporter (POT) 2.A.17.4.7	*Shewanella oneidensis*	2XUT	3.6	2011	Inward-facing, occluded
$PepT_{So2}$	Peptide:H^+ symporter	POT 2.A.17.4.7	*Shewanella oneidensis*	4LEP, 4TPH, 4TPG, 4TPJ	3.2	2013	Ligand-bound, inward open
$PepT_{St}$	Peptide:H^+ symporter	POT 2.A.17.1.6	*Streptococcus thermophilus*	4APS	3.3	2012	Inward open
GkPOT	Peptide:H^+ symporter	POT 2.A.17.1.7	*Geobacillus kaustophilus*	4IKV, 4IKW, 4IKX, 4IKY, 4IKZ	**1.9**	2013	Inward open
YbgH	Peptide:H^+ symporter	POT 2.A.17.1.4	*Escherichia coli*	4Q65	3.4	2014	Inward open
NRT1.1	Nitrate:H^+ symporter	POT 2.A.17.3.1	*Arabidopsis thaliana*	4OH3, 4CL4, 4CL5	3.25	2014	1. Apo inward open 2. Inward open with nitrate

*Bold text in cells indicates milestones in the study of MFS proteins. GLUT1 is the only human (*Homo sapiens*) MFS transporter for which a structure is available, 1.9 Å is the highest resolution among all MFS structures obtained to date, and 2003 is the year in which the first MFS structures were reported. Abbreviations: PDB, Protein Data Bank; TCDB, Transport Classification Database.

the structures were achieved using bacterial homologs, three came from eukaryotes: the human glucose transporter GLUT1 (14), the plant nitrate transporter NRT1.1 (82, 99), and a fungus phosphate transporter PiPT (83). GLUT1 represents the first and the only human SLC protein to have a known structure at an atomic resolution.

Another major breakthrough in the structural study of MFS transporters is the visualization of multiple conformations for one protein. Transporters undergo cycles of conformational shifts to achieve alternating access. Thus, obtaining structures of multiple conformations of a given protein has been an important goal for structural biologists seeking to understand its transport mechanism. The structures obtained for MFS transporters prior to 2013 did exhibit different conformations, but, unfortunately, the different conformations belonged to distinct transporters. Until 2013, none of the proteins had been captured in more than one conformational state (**Figure 2**) (115). Since then, however, structures for more than one conformational state of the D-xylose:proton symporter XylE (84, 110), LacY (60), the nitrate:nitrite antiporter NarU (114), and the melibiose:cation symporter MelB (19) have been obtained (**Table 2**).

This exciting progress has greatly advanced the mechanistic understanding of MFS proteins. In the next subsection, I review the common and distinct structural features of representative MFS transporters and the recent advancements in the structural elucidation of new MFS transporters. I then focus on GLUT1 and its bacterial homologs to discuss mechanistic insights.

General Structural Features of the Major Facilitator Superfamily

All of the MFS transporters share a common and characteristic core fold, known as the MFS fold (**Figure 3*a***).To facilitate a structural description of it, I introduce a coordinate system whereby the two axes parallel to the membrane plane and corresponding to the major and minor axes of the oval-shaped cross-section of the protein are defined as axes *a* and *b*, respectively, and the axis perpendicular to the membrane plane is axis *c* (**Figure 3*a***). A canonical MFS fold comprises two domains, each consisting of six consecutive TMs. The two domains, usually called the N and C domains, exhibit a twofold pseudosymmetry related by axis *c*. Within each domain, the six TMs are organized into a pair of inverted "3+3" repeats. In the N domain, TMs 1, 2, and 3 are related to TMs 4, 5, and 6 by an approximate 180° rotation around axis *a*; in the C domain, TMs 7, 8, and 9 have a similar relationship with TMs 10, 11, and 12 (**Figure 3*a***).

The corresponding TMs in each repeat appear to play similar structural and functional roles (115). The first helix in each three-helix bundle (TMs 1, 4, 7, and 10) is positioned in the center of the transporter, and together, these helices directly constitute the transport path (**Figure 3*a***). A large majority of the residues identified for substrate binding and cotransport coupling are located on these four helices. During a transport cycle, the interactions between TM1 and TM7 on the extracellular side occur in alternation with those between TM4 and TM10 on the cytoplasmic side to insulate the substrate binding site from the extramembrane milieu. Notably, although most of the TMs in MFS proteins are continuous helices, discontinuity occurs for TMs 1, 4, 7, and 10, possibly providing the structural adaptability needed for alternating access (14, 52, 100). TMs 2, 5, 8, and 11, which are positioned on the outside of the core helices along axis *b*, mediate the interface between the N and C domains. Residues in these segments that face the transport pathway may participate in substrate binding and cotransport coupling (100, 124). TMs 3, 6, 9, and 12 are placed on the outside of TMs 1, 4, 7, and 10 along axis *a*, supporting the structural integrity of the transporter (**Figure 3*a***). Interestingly, in the context of the overall structure, corresponding TMs from two three-TM repeats always stand next to each other in opposite orientations (**Figure 3*a***).

In addition to the core MFS fold, some members of the MFS may contain extra domains and motifs (**Figure 3*b***). For example, all of the structures of proteins in the sugar porter (SP) family have

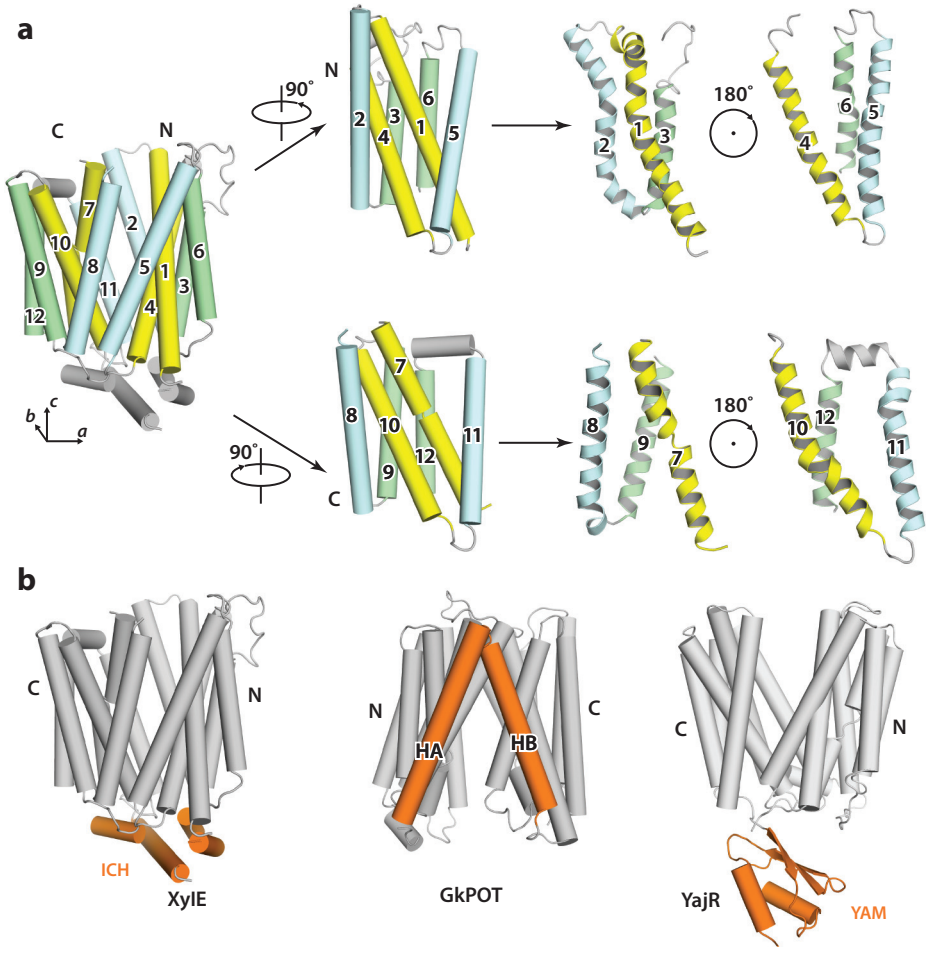

Figure 3

Structural features of the major facilitator superfamily (MFS) proteins. (*a*) A canonical MFS fold. The 12-TM structure in an MFS fold contains two discretely folded domains, the N and C domains, which are related by an approximate 180° rotation around axis *c* (defined at the bottom of the panel). Each domain consists of two inverted 3-TM repeats. The corresponding helices in each of these units have the same color. (*b*) Unique structural elements from distinct MFS subfamilies. Abbreviations: ICH, intracellular helical; MBD, methyl-CpG-binding domain protein 2; TM, transmembrane segment; YAM, YajR/AraEP/MBD.

an intracellular helical (ICH) domain, which comprises three or four helices between the N and C domains and one short helix at the C terminus. The ICH domain is essential for intracellular gating in XylE and GLUT1 (14, 79, 100). The structures of the bacterial peptide transporters from the proton-dependent oligopeptide transporter (POT) family all contain two extra TMs, designated HA and HB, which are inserted between the N and C domains. The inserted helical hairpin is missing in the POT protein NRT1.1 from *Arabidopsis thaliana*, supporting the conclusion that these extra TMs are not ubiquitous to proteins in the POT subfamily (12). Nevertheless, a recent study of the POT protein YbgH demonstrated that the internal rigidity of the helical hairpin is important for their transport activity (121). In the multidrug resistance transporter YajR, an independently

folded YAM [YajR/AraEP/ methyl-CpG-binding domain protein 2 (MBD)] domain follows the C-terminus of the TM domain, although the function of this soluble domain remains unclear (52).

Recent Progress in the Structural Study of the Major Facilitator Superfamily

A summary of the structural advances of MFS transporters prior to 2013 can be found in a minireview by Yan (115). Below is a brief review of the major achievements in structural biology of the MFS over the past two years. An inventory of all of the resolved MFS protein structures can be found in **Table 2**.

The sugar porter family: GLUT1 and its bacterial homologs XylE and GlcP. The glucose transporters GLUT1–GLUT4 represent some of the physiologically most important and most rigorously characterized transporters. Their significance in physiology and disease has been reviewed recently (74, 115) and is not discussed here. GLUTs have been the targets of active structural research for decades. However, the daunting challenges involved in working with eukaryotic membrane proteins have prevented any major progress on the structural determination of GLUTs (35). Before the crystal structure of human GLUT1 was elucidated in early 2014 (14), homology models of GLUTs were generated based on the crystal structures of their bacterial homolog, XylE.

GLUTs belong to the SP subfamily (**Table 2**), the members of which are responsible for the cellular uptake of glucose and other monosaccharides or disaccharides in all kingdoms of life (7, 39, 66, 81, 109). Among the bacterial homologs, XylE from *E. coli* shares ~30% sequence identity and ~50% similarity with human GLUT1–GLUT4. The crystal structure of XylE was first obtained in an outward-facing and partly occluded conformation, bound to its substrate, D-xylose; its inhibitor, D-glucose; and a glucose derivative, 6-bromo-6-deoxy-D-glucose, at resolutions of 2.8, 2.9, and 2.6 Å, respectively (100). Subsequently, two more conformations of XylE, the inward open and partly inward occluded conformations, were captured (84). Despite the relatively low resolution and severe anisotropy in X-ray diffraction, the backbones of these structures were clearly resolved. Thus, for the first time, the structures of both outward-facing and inward-facing conformations of the same MFS transporter were obtained, and XylE therefore became another prototypal MFS protein for structural and mechanistic examinations.

The structure of the inward open conformation of the D-glucose:proton symporter GlcP from *Staphylococcus epidermidis* was determined at a resolution of 3.2 Å (47). The structures of XylE and GlcP provide an important framework for mechanistic understanding of the SP transporters and for homology modeling of the physiologically more relevant GLUTs.

Finally, the crystal structure of the human GLUT1, which exhibits an inward open conformation, was determined at a resolution of 3.2 Å (**Figure 4*a***). Four key factors contributed to the success of GLUT1 structure determination (14). First, the previously identified glycosylation site N45 was substituted with threonine to prevent potential heterogeneity caused by glycosylation. Second, a single point mutation, E329Q, which was suggested to lock the transporter in an inward-facing state (92), was introduced to improve conformational homogeneity. Third, the crystallization trials were carried out at 4°C to stabilize the protein. Finally, the detergent nonyl-β-D-glucopyranoside (β-NG) was used in the last step of GLUT1 purification and crystallization. The electron density of a β-NG molecule could be unambiguously resolved in the structure. Interestingly, the glucoside of β-NG, which is reminiscent of D-glucose, is bound to the structure in a manner similar to the binding of D-glucose to XylE (**Figure 4*b***). Because of the chirality of glucoside and the presence of the aliphatic tail, the β-NG molecule can bind only to the inward-facing conformation of GLUT1. Therefore, the specific detergent molecule also contributes to the stabilization of the inward open conformation.

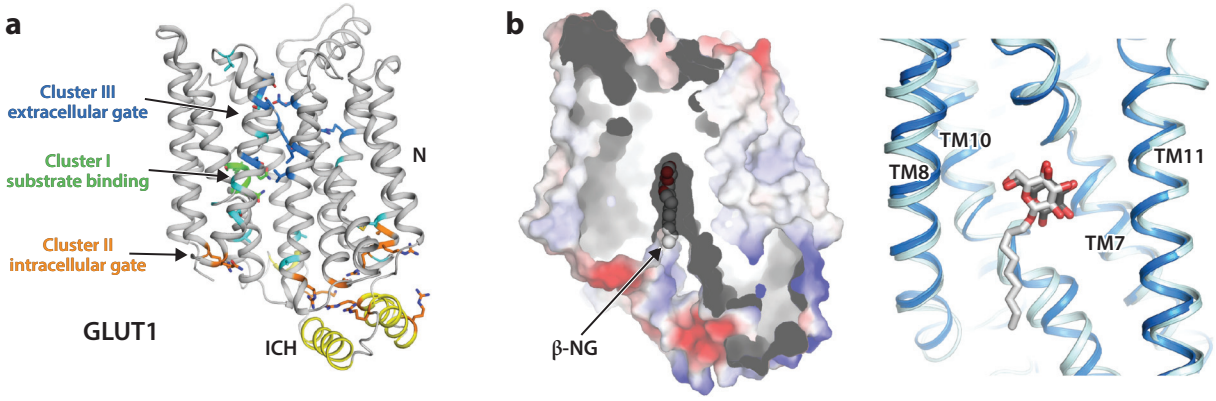

Figure 4

The structure of the human glucose transporter GLUT1 in an inward open conformation. (*a*) Mapping of disease-related mutations on the GLUT1 structure identified three clusters, which are important for substrate binding or for the extracellular or intracellular gating of GLUT1. (*b*) A molecule of the detergent β-NG is bound in the central cavity. The coordination of the sugar moiety of β-NG by GLUT1 is similar to the binding of D-glucose by XylE. The structures of GLUT1 (*blue*) and XylE (*pale cyan*) are superimposed relative to their respective C domains. The ligands are shown using stick diagrams. Abbreviations: β-NG, nonyl-β-D-glucopyranoside; ICH, intracellular helical domain.

The GLUT1 structure allows mapping of over 40 mutations associated with GLUT1 deficiency syndrome (also known as De Vivo syndrome) (14). These mutations are predominantly clustered in three regions. Cluster I overlaps with the substrate binding site; cluster II mediates the interactions between the TM domain and the ICH domain, contributing to the closure of the intracellular gate; and cluster III is involved in the contacts between the N and C domains on the extracellular side, representing the extracellular gate. Structure-guided analysis of disease-related mutations thus facilitates mechanistic understanding of both GLUT1 and the SP proteins in general (14) (**Figure 4*a***).

The aforementioned ICH domain is observed in all SP structures, indicating that this domain is a general feature of the SP subfamily. The SP transporters share several conserved signature motifs (38, 70, 84, 100), which are exclusively positioned on the cytoplasmic side of the structure, lining up the interface between the TM and ICH domains and supporting an essential functional role of the ICH domain. Structural comparison suggests that the ICH domain may serve as a latch to stabilize the outward-facing conformation of the transporter (14, 100).

The proton-dependent oligopeptide transporter family: GkPOT and NRT1.1. The POT or PTR family comprises proton symporters that catalyze the cellular uptake of short peptides. A subfamily in plants, exemplified by NRT1.1, permeates nitrogenous ligands (65). Importantly, the human SLC15 POT proteins PepT1 and PepT2 have direct pharmaceutical relevance through uptake of a variety of drugs (96). Thus, proteins belonging to the POT family have been actively pursued for structural characterizations. With the exception of the nitrate transporter from *Arabidopsis thaliana*, NRT1.1, the POT structures obtained to date are for a number of bacterial homologs, including $PepT_{So}$ (77), $PepT_{St}$ (97), $PepT_{So2}$ (31, 32), GkPOT (15), and YbgH (121) (**Table 2**).

A comprehensive review on the structural biology of the POT/PTR family was published recently (76). Here, I would like to bring particular attention to the structure of GkPOT, a peptide:proton symporter in *Geobacillus kaustophilus*. The crystals were obtained in the lipidic

cubic phase (LCP), and the diffraction reached 1.9 Å (15). The structure can be superimposed well with other bacterial POT homologs for which crystals were obtained in detergent micelles, partially alleviating the concern that the structures of a membrane transporter may be distorted by detergents.

NRT1.1 is the only plant MFS protein for which detailed structural information is available (82, 99). This protein exhibits dual affinities for nitrate. The phosphorylation of T101 serves as the signal to switch from a low-affinity to a high-affinity state. Interestingly, the structure of NRT1.1 revealed a dimeric assembly in the crystal. Zheng and coworkers (122) examined the oligomerization status of NRT1.1 in a detergent solution by cross-linking and in oocyte membranes by Förster resonance energy transfer (FRET) spectroscopy analysis. The dimerization of wild-type NRT1.1 was confirmed in both experiments. Furthermore, a phosphomimetic mutant of NRT1.1, T101D, which exhibits high-affinity nitrate transport activity, was shown to be a monomer in the lipid bilayer. These studies established the correlations between the phosphorylation and oligomerization states of NRT1.1 (99). Whether disruption of the dimer interface without phosphorylation of T101 is sufficient to convert NRT1.1 from the low-affinity to the high-affinity state remains to be studied.

Other families: the PHS, NNP, and GPH subfamilies. The structural gallery of MFS proteins has been expanded to contain more subfamilies, including the phosphate:H^+ symporter family (PHS), the nitrate:nitrite porter family (NNP), and the glycoside-pentoside-hexuronide:cation symporter (GPH) family (**Table 2**).

The phosphate:H^+ symporter PiPT, from the fungus *Piriformospora indica*, represents the first eukaryotic MFS protein for which an atomic structure was obtained. The structure was captured in a ligand-bound, inward occluded state at a resolution of 2.9 Å and serves as a framework for the elucidation of the substrate binding and proton coupling mechanism (83).

The structures of the nitrate:nitrite antiporters NarU and NarK from *E. coli* were determined at resolutions of 3.0 and 2.6 Å, respectively (114, 122). Both proteins were captured in inward-facing conformations. Each asymmetric unit of the NarU crystal contains two molecules, one in the occluded conformation and the other in a partially inward open state (114). The structures of NarK were also obtained in two inward open states: ligand-free and phosphate-bound (122). The NNP structures in three distinct conformational states provide insights into their functional mechanisms.

A crystal structure of the melibiose permease MelB in *Salmonella typhimurium* was obtained at a resolution of 3.4 Å (19). The four molecules in each asymmetric unit exhibit two conformations, the partly outward occluded conformation and the outward inactive conformation. Notably, MelB can catalyze the symport of melibiose with Na^+, Li^+, or H^+. Structural analysis identified a trigonal bipyramid geometry, composed of the D55/59/124 and Y120/T121/T373 side chains, as a potential cation binding site. Replacing any of the residues at positions 55/59/121/124 with cysteine led to altered cation selectivity, supporting the notion of the geometry described above as a cation binding site. The structures of MelB provide a framework for understanding the coupling and alternating-access mechanism of the MFS Na^+ symporters.

LacY. LacY has been a prototype for the study of secondary transporters. After its first structure (an inward open conformation) was determined, a decade of rigorous effort failed to capture another conformation. The breakthrough was finally made in early 2014. Through rational design, two conserved residues, G46 and G262, located on the extracellular segments of TM2 and TM8, respectively, were replaced by tryptophan residues. These two residues are positioned on the interface between the N and C domains. Substitution of glycine with a bulky residue is

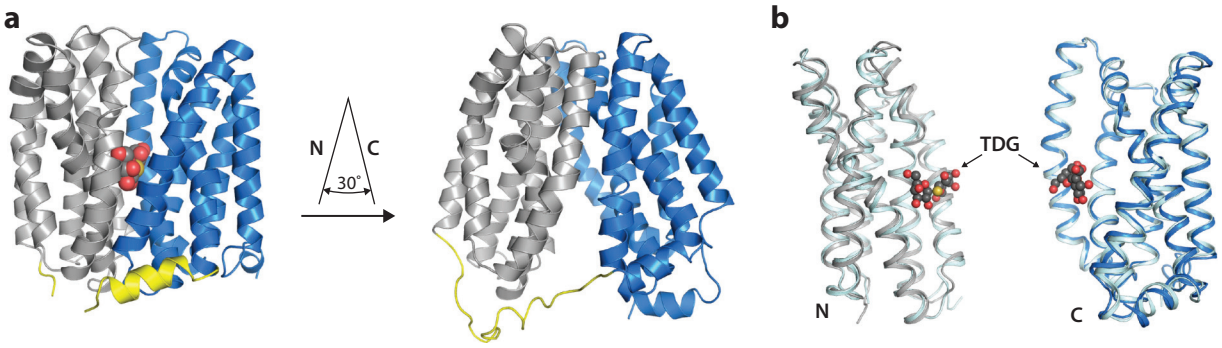

Figure 5

State transition of LacY is achieved via rigid-body rotation of the two domains. (*a*) Structural comparison of LacY between the TDG-bound, nearly occluded, outward-facing conformation (*left*) and the inward open conformation (*right*). A 30° concentric rotation around axis *b* (see **Figure 3*a***) results in the transition from the outward occluded to inward open state. (*b*) Domain superimposition of the two structures of LacY. The N and C domains in the two structures exhibit almost identical conformations, supporting the notion of a rigid-body rotation of the two domains. Abbreviation: TDG, D-galactopyranosyl-1-thio-β, D-galactopyranoside.

predicted either to open the interface of the two domains on the extracellular side or to destabilize the inward open conformation. Indeed, the structure of the tryptophan-modified LacY variant (G46W/G262W) exhibits a ligand-bound and almost occluded outward-facing conformation (**Figure 5*a***) (60). The conformational shift from the outward occluded state to an inward open one involves a 30°concentric rotation of the two domains around axis *b* (**Figures 3*a*** and **5*a***). Pairwise superimposition of the respective N and C domains suggests a rigid-body rotation of the two domains during the conformational shift (**Figure 5*b***).

STRUCTURE-GUIDED MECHANISTIC ELUCIDATION

Structural information lays out the foundation for mechanistic investigations. Three fundamental mechanisms need to be addressed for all of the MFS transporters: the molecular basis underlying substrate selectivity; the conformational changes that take place during an alternating-access cycle; and, most importantly, the coupling mechanisms for antiporters and symporters. The exciting progress in the structural elucidation of MFS proteins in the past couple of years has further advanced our understanding of these fundamental mechanisms.

Substrate Binding

The structurally elucidated MFS transporters all contain a single substrate binding cavity located in the center of the membrane and enclosed by the N and C domains. Before their ligand-bound structures were determined, many MFS transporters were subjected to mutagenesis to identify residues that recognize substrate; examples of some of the transporters studied are LacY, GalP, FucP, and $PepT_{St}$ (115). Structures of XylE in complex with three different ligands revealed the first picture of substrate coordination by an MFS transporter (100), and structures of substrate-bound transporters were subsequently resolved for PiPT, NarK, LacY, and $PepT_{So2}$. These structures reveal two common features: Multiple aromatic residues are positioned surrounding the trapped substrate, insulating it from the extramembrane environment, and the ligands are usually asymmetrically coordinated by the two domains.

In all MFS symporters and facilitators with known ligand-bound structures, it appears that one domain provides the primary binding site, whereas the other contributes few coordinating residues. For example, in the partly outward occluded conformation of XylE, the bound ligand is predominantly coordinated by the C domain, and the N domain contributes only three binding residues (100). In the inward open GLUT1 structure, the glucoside of β-NG is exclusively coordinated by residues from the C domain in a manner almost identical to the coordination of D-glucose by XylE (**Figure 4*b***) (14). In the inward occluded PiPT structure, the bound phosphate is closer to the C domain and is coordinated by six residues from the C domain and by only two from the N domain (83). In the outward occluded LacY structure, the bound ligand is closer to the N domain, which provides more coordinating residues than the C domain does. Therefore, the N domain appears to serve as the primary substrate binding site in LacY (60). In the recently reported peptide-bound inward open $PepT_{So2}$ structure, the tripeptide is also coordinated mainly by residues in the N domain (31).

The only exception to date is seen in the structure of nitrite-bound NarK, in which the two domains appear to contribute equally to substrate binding. Note that NarK is an antiporter, whereas the others mentioned above are all symporters. It remains to be further investigated whether the observed patterns of substrate binding, which are asymmetric for symporters and symmetric for antiporters, can be generalized to other MFS proteins, and if so, whether such patterns are associated with the transport mechanisms of antiporters and symporters.

Alternating Access

Multiple conformations for each MFS transporter, which have been observed for several distinct proteins, provide the framework for a mechanistic understanding of alternating access. Mounting evidence has demonstrated that the state transitions for an MFS protein involve both domain rotation and local structural rearrangements. For LacY, the transition from the outward occluded to the inward open state requires a 30° rigid-body rotation of the two domains. In XylE, NarU (114), and MelB (19), however, local structural rearrangements of specific TMs are observed between distinct states. I discuss XylE as a representative example because it has been captured in three distinct conformations (**Figure 6**)

For XylE, the transition from the ligand-bound, partly outward occluded state to the inward open state requires an approximately 16° concentric domain rotation around axis *b* (**Figure 6*a***). Meanwhile, structural rearrangements occur in the extracellular segment of TM7, the cytoplasmic fragment of TM10, and in the cytoplasmic fragment and extracellular tip of TM11 (**Figure 6*b***). Interestingly, the N domain remains unaltered during the state transition. Because the C domain provides the primary substrate binding site for XylE, the local conformational changes of the C domain involving TM7 and TM10 may be associated with substrate binding and release. The rigid-body rotation of the N domain results in the alternative exposure of the substrate binding site to one side of the membrane or the other (14).

A partly inward occluded state was captured in the absence of ligand for XylE (84). Comparison with the inward open structure reveals a local bending of TM10 on the cytoplasmic side toward the central cavity, resulting in the partly occluded state (**Figure 6*c***). Similar conformational changes were observed between the inward open $PepT_{St}$ (77) and the inward occluded $PepT_{So}$ (77). These structural observations suggest that the conformational rearrangements underlying an alternating-access cycle are more complex than a simple rigid-body rotation, or the so-called rocker-switch model (46). XylE has become a prototypal protein for the study of alternating access. A complete picture of the alternating-access cycle for XylE relies on successful determination of the structure of XylE in its outward open state.

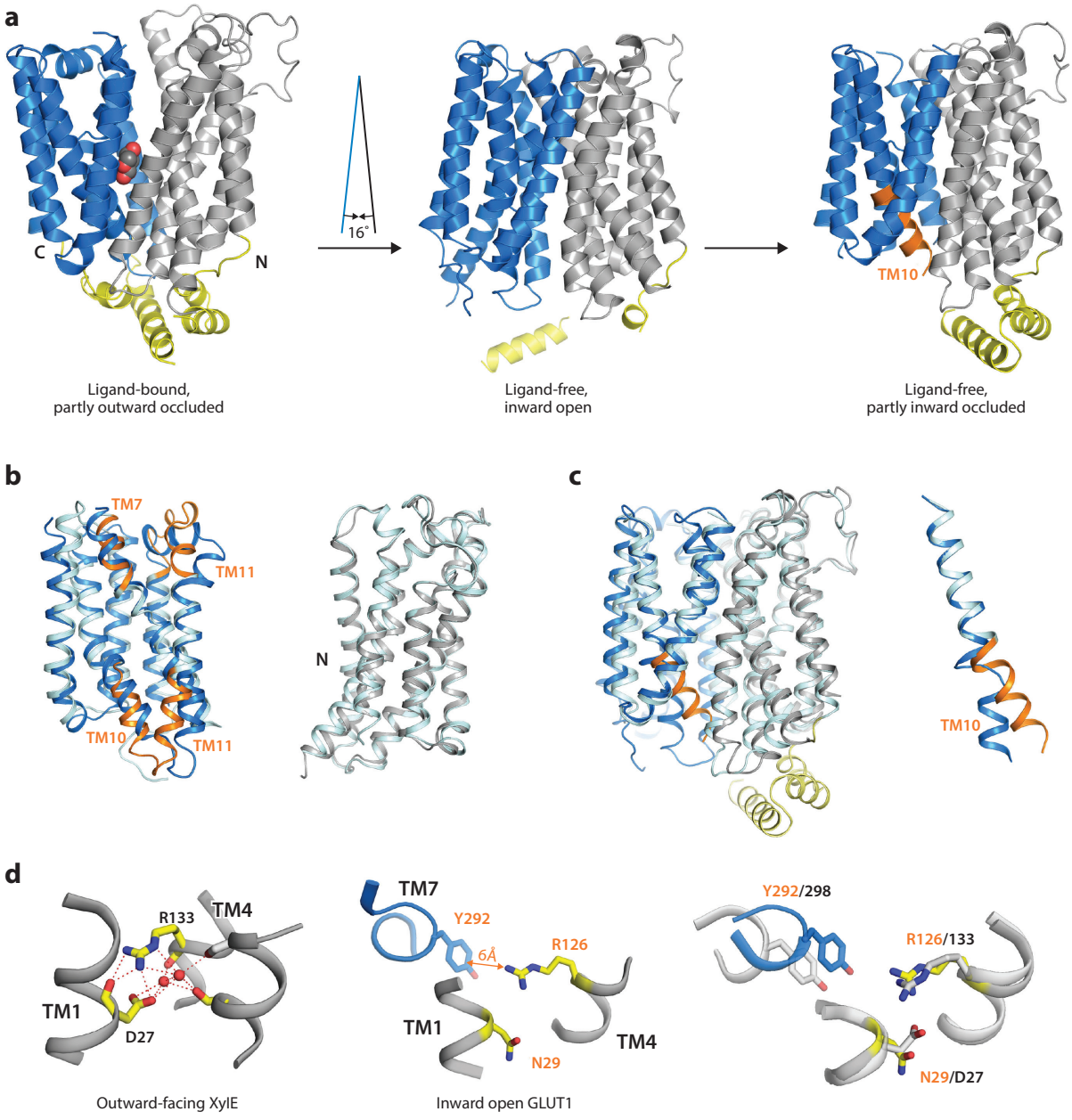

Figure 6

Alternating-access and proton coupling mechanisms of XylE. (*a*) Structures of XylE in three conformations. PDB IDs for the three structures are as follows: 4GBY (*left*), 4QIQ (*middle*), and 4JA3 (*right*). (*b*) Superimpositions of the individual domains between the outward-facing and inward open states. The inward open XylE is colored in pale cyan in panels *b* and *c*. The regions with local conformational shifts are highlighted in orange. (*c*) Structural comparison of the inward open and partly inward occluded states of XylE. The only difference occurs in the cytoplasmic segment of TM10, which is highlighted on the right. (*d*) Structural comparison of the outward-facing conformation of XylE with the inward open conformation of GLUT1. The hydrogen bonds are represented by red dashed lines. The rightmost illustration depicts the superimposed structures of GLUT1 and XylE relative to their respective N domains. Abbreviation: TM, transmembrane segment.

The Coupling Mechanism of Major Facilitator Superfamily Proton Symporters

The coupling mechanism through which an active transporter utilizes the energy released from the downhill translocation of one substrate to drive the uphill movement of the other remains mostly enigmatic. Among the secondary active transporters, the proton symporters have been relatively well characterized (116). The understanding of the coupling mechanism for MFS proton symporters prior to 2012 has already been summarized in several reviews (22, 54, 115). Here, I focus on some recent discoveries that may facilitate mechanistic interpretation of proton coupling in SP proton symporters.

An aspartic acid residue at position 27 of XylE (69), which corresponds to D32 in the galactose:proton symporter GalP (91) and D22 in GlcP (47), plays a critical role in proton coupling. The mutation D27N in XylE, or D22N in GlcP, led to elimination of proton-dependent active symport, but not counterflow activity (47, 69). The mechanism by which D27 of XylE and the corresponding aspartic acid residues in the other SP proteins affect the coupling remained largely unknown until the structural determination of GLUT1, which revealed a tantalizing clue.

In the outward-facing XylE structure (100), D27 on TM1 forms a network of hydrogen bonds with the invariant R133 on TM4 (**Figure 6*d***). This structure was obtained at pH 9.5, suggesting that D27 may be deprotonated. In the inward open GLUT1 structure, N29, which corresponds to D27 of XylE, mimics a permanently protonated state of aspartic acid. It is of particular note that R126 of GLUT1, which corresponds to R133 of XylE, does not interact with N29 (**Figure 6*d***). Thus, one can reasonably speculate that in XylE, upon protonation of D27, the side chain of R133 would be released, possibly triggering the outward-to-inward transition. Note that the guanidinium group of R126 in GLUT1 is approximately 6 Å away from the benzene ring of Y292, so these groups likely form cation–π interactions in the inward open GLUT1 (**Figure 6*d***). In the outward-facing XylE, the aromatic ring of Y298, which corresponds to Y292 of GLUT1, is approximately 9 Å away from the guanidinium group of R133, placing these residues too far apart for cation–π interactions (**Figure 6*d***). Therefore, a comparison of the facilitator GLUT1 and the proton symporter XylE provides an important clue to understanding the proton coupling mechanism.

Uniporters catalyze only the translocation of a substrate down its concentration gradient (**Figure 1**). The conformational switches of the transporters are the key to completing a transport cycle. In GLUT1, the ligand-free protein may prefer an outward open conformation because of the extensive interactions between the TM and ICH domains (**Figure 4*a***). Substrate binding at the central site on the C domain may induce closure of the N and C domains on the extracellular side, leading to a rearrangement of interactions on both sides of the bound substrate. When the binding affinity between the N and C domains on the extracellular side of the membrane exceeds that on the intracellular side, the protein may switch to the inward open conformation. Once GLUT1 adopts the inward open conformation, the substrate is exposed to a low-concentration milieu, and the equilibrium shifts toward substrate dissociation. The empty uniporter then returns to the outward-facing conformation (**Figure 7**).

For proton-driven symporters, the translocation of proton and substrate are obligatorily coupled. The general transport mechanism of a proton-coupled symporter such as XylE may be similar to that of the uniporter if the substrate (xylose) and the obligatory ligand (proton) are considered as a single entity (**Figure 7**). Because there are two types of substrates, however, the key difference between a symporter and a facilitator is that the translocation of one substrate (sugar or H^+) cannot be completed without that of the other. The detailed mechanism of the complete transport cycle awaits further characterization, but this analysis provides a tentative answer to one step of the cycle for XylE. In the absence of H^+, arrival of the sugar induces the closure of the N and C domains, but the protein cannot complete the outward-to-inward transition because the

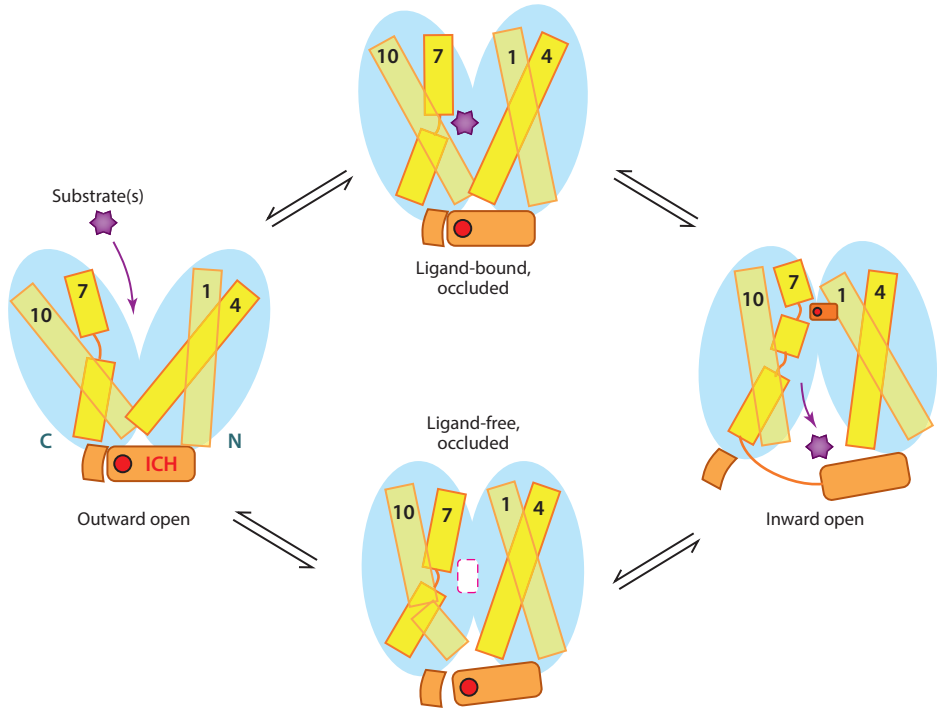

Figure 7

A working model for the sugar porter (SP) family, showing a revised version of the alternating-access model in **Figure 2**. The outward open structure remains to be determined, but the other conformations are derived from the appropriate XylE and GLUT1 structures. The intracellular helical domain (ICH) is illustrated as a latch that strengthens the intracellular gate in the outward open conformation. The extracellular gate comprises a few residues from TM1, TM4, and TM7, which are illustrated by the red zone in the inward open cartoon. Substrate(s) refers to one solute in facilitators and to two cotransported chemicals in symporters. Abbreviation: TM, transmembrane segment.

switch, namely residue R133, is sequestered by deprotonated D27 (**Figure *6d***). Protonation of D27 releases R133, which may subsequently reach out to interact with the C domain and thereby trigger the outward-to-inward transition. In the inward-facing conformation, the equilibrium may be shifted toward deprotonation because the environment has a low proton concentration. Deprotonation may be an essential step for the release of the substrate into a high-concentration environment. The deprotonated and substrate-released transporter then returns to the outward open conformation.

Many detailed mechanisms, such as the translocation route and the alternating-access mechanism for H^+, remain to be investigated. In addition, one key element that distinguishes symporters from uniporters remains unclear—the inward open, substrate-released symporter cannot return to the outward-facing conformation without deprotonation, whereas a uniporter can achieve this switch despite its permanently protonated state. Further experimental characterizations, as well as molecular dynamics (MD) simulations, are likely required to address these remaining issues.

PERSPECTIVE

The exciting progress in the structural elucidation of MFS transporters in recent years has provided significant insights into our understanding of their mechanisms of activity. Despite these advances,

however, several important issues remain to be addressed. Four examples of these issues are discussed in the following subsections.

Structural Determination of Additional Major Facilitator Superfamily Subfamilies

As summarized in **Table 2**, the 18 MFS proteins whose structures have been reported so far belong to nine families. However, the structures of most MFS families, especially those of families with significant physiological and pharmaceutical relevance such as the vesicular glutamate or amine transporters, are yet to be resolved (**Table 1**). Although all MFS proteins share a common structural fold, the unique features of specific families may support their specific biological functions. Obtaining the atomic structure for MFS members that have been identified as drug targets is of particular importance. The information provided by the homologous models, especially those of distantly related proteins, may not be sufficient for structure-guided drug design. Therefore, structural determination of the MFS members that are of direct physiological and pharmaceutical relevance represents one major direction for the study of the structural biology of MFS proteins in the future.

Elucidation of the Major Facilitator Superfamily Transport Mechanism

Although structures of multiple conformations are available for XylE and a few other MFS proteins, there is inadequate information on any MFS transporter to propose a complete alternating-access cycle. The outward open conformational state is still missing for XylE. A multitude of techniques, including the introduction of specific point mutations (14, 29, 60), chemical cross-linking (21, 80, 88), and cocrystallization with binders such as antibodies or nanobodies (86, 98), have been developed and have proven useful for facilitating the generation and structural determination of a desired conformation.

The revolutionary advances in cryo electron microscopy (cryoEM) are reshaping structural biology. The structures of extremely challenging targets for crystallography (59), exemplified by the ion channel TRPV1 (8, 67) and the membrane complex γ-secretase, were resolved by cryoEM at reasonable resolutions (68). CryoEM also has the advantage of revealing multiple conformations of the target macromolecules through classification (72). Whether high-resolution structural determination of the MFS proteins, for which monomers have an average molecular weight of approximately 50 kDa, can be reliably performed by single-particle cryoEM analysis remains to be seen.

In addition to capturing a complete alternating-access cycle, the coupling mechanism remains the most intriguing and challenging unresolved issue in the study of MFS symporters and antiporters. Elucidation of the coupling mechanism may require combination of multiple approaches. Finally, kinetic investigations of the transport process represent another challenging aspect for the mechanistic understanding of MFS proteins.

Modulation of Major Facilitator Superfamily Proteins by Lipids

During protein purification and crystallization, the native environment for membrane proteins—the lipid bilayer—is destroyed. This presents a challenge for researchers seeking to better understand the behavior of MFS proteins, as the surrounding lipids are an integral component for the structure and function of a membrane transporter. However, the study of the modulation of membrane proteins by lipids has been a grave challenge, owing to the difficulty of dealing with

lipid molecules. Because an MFS transporter undergoes a large degree of conformational change during the alternating-access cycle, the surrounding lipids in their native environment are likely to affect the function, kinetics, or even thermodynamics of the transporter. The modulation of MFS transporters by specific lipids has yet to be systematically explored. Development and application of new technologies are required to advance our understanding of the interactions between integral membrane proteins and their surrounding lipids (61).

Deorphanization of Major Facilitator Superfamily Members

Despite rapid progress in the structural and mechanistic understanding of MFS transporters, an important aspect of their study remains, namely, characterization of the functions of many MFS proteins. Even for the rigorously characterized human proteins (**Table 1**), the physiological function, localization, and substrates for the majority of the SLC transporters, including GLUT6–GLUT14, remain largely enigmatic. Consequently, most of the MFS members are still orphan transporters. For example, an MFS member in mice, Mfsd2a, was only recently identified as an essential transporter for the omega-3 fatty acid decosahexaeoic acid (78). Together, the deorphanization and annotation of MFS members, especially those in humans and mammals, represent a major challenge for the future study of the MFS.

DISCLOSURE STATEMENT

The author is not aware of any affiliations, memberships, funding, or financial holdings that might be perceived as affecting the objectivity of this review.

ACKNOWLEDGMENTS

I thank Dr. Liang Feng, Dr. Brendan Lehnert, Dr. Yigong Shi, and Dr. Ting Zhu for critical reading of the article. This work was supported by funds from the Ministry of Science and Technology of China (2015CB910101) and from the National Natural Science Foundation of China (31125009). The research of N.Y. was supported in part by an International Early Career Scientist grant from the Howard Hughes Medical Institute and by an endowed professorship from Bayer Healthcare.

LITERATURE CITED

1. Abramson J, Smirnova I, Kasho V, Verner G, Kaback HR, Iwata S. 2003. Structure and mechanism of the lactose permease of *Escherichia coli*. *Science* 301:610–15
2. Agre P. 2004. Aquaporin water channels. *Biosci. Rep.* 24:127–63
3. Almén MS, Nordström KJ, Fredriksson R, Schiöth HB. 2009. Mapping the human membrane proteome: a majority of the human membrane proteins can be classified according to function and evolutionary origin. *BMC Biol.* 7:50
4. Bang O, Orskov SL. 1937. Variations in the permeability of the red blood cells in man, with particular reference to the conditions obtaining in pernicious anemia. *J. Clin. Investig.* 16:279–88
5. Birnbaum MJ, Haspel HC, Rosen OM. 1986. Cloning and characterization of a cDNA encoding the rat brain glucose-transporter protein. *PNAS* 83:5784–88
6. Bodoy S, Fotiadis D, Stoeger C, Kanai Y, Palacín M. 2013. The small SLC43 family: facilitator system l amino acid transporters and the orphan EEG1. *Mol. Asp. Med.* 34:638–45
7. Büttner M. 2007. The monosaccharide transporter(-like) gene family in *Arabidopsis*. *FEBS Lett.* 581:2318–24

8. Cao E, Liao M, Cheng Y, Julius D. 2013. TRPV1 structures in distinct conformations reveal activation mechanisms. *Nature* 504:113–18
9. Chou JY, Jun HS, Mansfield BC. 2013. The SLC37 family of phosphate-linked sugar phosphate antiporters. *Mol. Asp. Med.* 34:601–11
10. Costa C, Dias PJ, Sá-Correia I, Teixeira MC. 2014. MFS multidrug transporters in pathogenic fungi: Do they have real clinical impact? *Front. Physiol.* 5:197
11. Dang S, Sun L, Huang Y, Lu F, Liu Y, et al. 2010. Structure of a fucose transporter in an outward-open conformation. *Nature* 467:734–38
12. Daniel H, Spanier B, Kottra G, Weitz D. 2006. From bacteria to man: archaic proton-dependent peptide transporters at work. *Physiology* 21:93–102
13. DeLano WL. 2002. The PyMOL Molecular Graphics System. **http://www.pymol.org**
14. Deng D, Xu C, Sun P, Wu J, Yan C, et al. 2014. Crystal structure of the human glucose transporter GLUT1. *Nature* 510:121–25
15. Doki S, Kato HE, Solcan N, Iwaki M, Koyama M, et al. 2013. Structural basis for dynamic mechanism of proton-coupled symport by the peptide transporter POT. *PNAS* 110:11343–48
16. Dos Santos SC, Teixeira MC, Dias PJ, Sá-Correia I. 2014. MFS transporters required for multidrug/multixenobiotic (MD/MX) resistance in the model yeast: understanding their physiological function through post-genomic approaches. *Front. Physiol.* 5:180
17. Ehring R, Beyreuther K, Wright JK, Overath P. 1980. In vitro and in vivo products of *E. coli* lactose permease gene are identical. *Nature* 283:537–40
18. El-Gebali S, Bentz S, Hediger MA, Anderle P. 2013. Solute carriers (SLCs) in cancer. *Mol. Asp. Med.* 34:719–34
19. Ethayathulla AS, Yousef MS, Amin A, Leblanc G, Kaback HR, Guan L. 2014. Structure-based mechanism for Na^+/melibiose symport by MelB. *Nat. Commun.* 5:3009
20. Finn RD, Bateman A, Clements J, Coggill P, Eberhardt RY, et al. 2014. Pfam: the protein families database. *Nucleic Acids Res.* 42:D222–30
21. Fluman N, Ryan CM, Whitelegge JP, Bibi E. 2012. Dissection of mechanistic principles of a secondary multidrug efflux protein. *Mol. Cell* 47:777–87
22. Forrest LR, Krämer R, Ziegler C. 2011. The structural basis of secondary active transport mechanisms. *Biochim. Biophys. Acta* 1807:167–88
23. Fox CF, Carter JR, Kennedy EP. 1967. Genetic control of the membrane protein component of the lactose transport system of *Escherichia coli*. *PNAS* 57:698–705
24. Fox CF, Kennedy EP. 1965. Specific labeling and partial purification of the M protein, a component of the β-galactoside transport system of *Escherichia coli*. *PNAS* 54:891–99
25. Fukumoto H, Kayano T, Buse JB, Edwards Y, Pilch PF, et al. 1989. Cloning and characterization of the major insulin-responsive glucose transporter expressed in human skeletal muscle and other insulin-responsive tissues. *J. Biol. Chem.* 264:7776–79
26. Fukumoto H, Seino S, Imura H, Seino Y, Eddy RL, et al. 1988. Sequence, tissue distribution, and chromosomal localization of mRNA encoding a human glucose transporter-like protein. *PNAS* 85:5434–38
27. Gadsby DC. 2009. Ion channels versus ion pumps: the principal difference, in principle. *Nat. Rev. Mol. Cell Biol.* 10:344–52
28. Gao X, Lu F, Zhou L, Dang S, Sun L, et al. 2009. Structure and mechanism of an amino acid antiporter. *Science* 324:1565–68
29. Gao X, Zhou L, Jiao X, Lu F, Yan C, et al. 2010. Mechanism of substrate recognition and transport by an amino acid antiporter. *Nature* 463:828–32
30. Guan L, Kaback HR. 2006. Lessons from lactose permease. *Annu. Rev. Biophys. Biomol. Struct.* 35:67–91
31. Guettou F, Quistgaard EM, Raba M, Moberg P, Low C, Nordlund P. 2014. Selectivity mechanism of a bacterial homolog of the human drug-peptide transporters PepT1 and PepT2. *Nat. Struct. Mol. Biol.* 21:728–31
32. Guettou F, Quistgaard EM, Tresaugues L, Moberg P, Jegerschold C, et al. 2013. Structural insights into substrate recognition in proton-dependent oligopeptide transporters. *EMBO Rep.* 14:804–10

33. Hagenbuch B, Stieger B. 2013. The *SLCO* (former *SLC21*) superfamily of transporters. *Mol. Asp. Med.* 34:396–412
34. Halestrap AP. 2013. The *SLC16* gene family—structure, role and regulation in health and disease. *Mol. Asp. Med.* 34:337–49
35. He Y, Wang K, Yan N. 2014. The recombinant expression systems for structure determination of eukaryotic membrane proteins. *Protein Cell* 5:658–72
36. Hediger MA. 1994. Structure, function and evolution of solute transporters in prokaryotes and eukaryotes. *J. Exp. Biol.* 196:15–49
37. Hediger MA, Clémençon B, Burrier RE, Bruford EA. 2013. The ABCs of membrane transporters in health and disease (SLC series): introduction. *Mol. Asp. Med.* 34:95–107
38. Henderson PJ, Maiden MC. 1990. Homologous sugar transport proteins in *Escherichia coli* and their relatives in both prokaryotes and eukaryotes. *Philos. Trans. R. Soc. Lond. B* 326:391–410
39. Henderson PJF, Baldwin SA. 2012. Structural biology: bundles of insights into sugar transporters. *Nature* 490:348–50
40. Heymann JAW, Sarker R, Hirai T, Shi D, Milne JLS, et al. 2001. Projection structure and molecular architecture of OxlT, a bacterial membrane transporter. *EMBO J.* 20:4408–13
41. Hirabayashi Y, Nomura KH, Nomura K. 2013. The acetyl-CoA transporter family SLC33. *Mol. Asp. Med.* 34:586–89
42. Hirai T, Heymann JAW, Shi D, Sarker R, Maloney PC, Subramaniam S. 2002. Three-dimensional structure of a bacterial oxalate transporter. *Nat. Struct. Biol.* 9:597–600
43. Hodgkin AL, Huxley AF. 1945. Resting and action potentials in single nerve fibres. *J. Physiol.* 104:176–95
44. Höglund PJ, Nordström KJV, Schiöth HB, Fredriksson R. 2011. The solute carrier families have a remarkably long evolutionary history with the majority of the human families present before divergence of Bilaterian species. *Mol. Biol. Evol.* 28:1531–41
45. Hruz PW, Mueckler MM. 2001. Structural analysis of the GLUT1 facilitative glucose transporter. *Mol. Membr. Biol.* 18:183–93
46. Huang Y, Lemieux MJ, Song J, Auer M, Wang DN. 2003. Structure and mechanism of the glycerol-3-phosphate transporter from *Escherichia coli*. *Science* 301:616–20
47. Iancu CV, Zamoon J, Woo SB, Aleshin A, Choe JY. 2013. Crystal structure of a glucose/H^+ symporter and its mechanism of action. *PNAS* 110:17862–67
48. Jacob F, Monod J. 1961. Genetic regulatory mechanisms in the synthesis of proteins. *J. Mol. Biol.* 3:318–56
49. Jacob F, Perrin D, Sanchez C, Monod J. 1960. Operon: a group of genes with the expression coordinated by an operator. *C. R. Hebd. Seances Acad. Sci.* 250:1727–29
50. James DE, Brown R, Navarro J, Pilch PF. 1988. Insulin-regulatable tissues express a unique insulin-sensitive glucose transport protein. *Nature* 333:183–85
51. Jardetzky O. 1966. Simple allosteric model for membrane pumps. *Nature* 211:969–70
52. Jiang D, Zhao Y, Wang X, Fan J, Heng J, et al. 2013. Structure of the YajR transporter suggests a transport mechanism based on the conserved motif A. *PNAS* 110:14664–69
53. Kaback HR, Sahin-Tóth M, Weinglass AB. 2001. The kamikaze approach to membrane transport. *Nat. Rev. Mol. Cell Biol.* 2:610–20
54. Kaback HR, Smirnova I, Kasho V, Nie Y, Zhou Y. 2011. The alternating access transport mechanism in LacY. *J. Membr. Biol.* 239:85–93
55. Kaback HR, Stadtman ER. 1966. Proline uptake by an isolated cytoplasmic membrane preparation of *Escherichia coli*. *PNAS* 55:920–27
56. Kasahara M, Hinkle PC. 1976. Reconstitution of D-glucose transport catalyzed by a protein fraction from human erythrocytes in sonicated liposomes. *PNAS* 73:396–400
57. Kasahara M, Hinkle PC. 1977. Reconstitution and purification of the D-glucose transporter from human erythrocytes. *J. Biol. Chem.* 252:7384–90
58. Koepsell H. 2013. The SLC22 family with transporters of organic cations, anions and zwitterions. *Mol. Asp. Med.* 34:413–35
59. Kühlbrandt W. 2014. Microscopy: Cryo-EM enters a new era. *eLIFE* 3:e03678

60. Kumar H, Kasho V, Smirnova I, Finer-Moore JS, Kaback HR, Stroud RM. 2014. Structure of sugar-bound LacY. *PNAS* 111:1784–88
61. Laganowsky A, Reading E, Allison TM, Ulmschneider MB, Degiacomi MT, et al. 2014. Membrane proteins bind lipids selectively to modulate their structure and function. *Nature* 510:172–75
62. Lawal HO, Krantz DE. 2013. SLC18: vesicular neurotransmitter transporters for monoamines and acetylcholine. *Mol. Asp. Med.* 34:360–72
63. Lee C, Kang HJ, von Ballmoos C, Newstead S, Uzdavinys P, et al. 2013. A two-domain elevator mechanism for sodium/proton antiport. *Nature* 501:573–77
64. LeFevre PG. 1948. Evidence of active transfer of certain non-electrolytes across the human red cell membrane. *J. Gen. Physiol.* 31:505–27
65. Léran S, Varala K, Boyer J-C, Chiurazzi M, Crawford N, et al. 2014. A unified nomenclature of NITRATE TRANSPORTER 1/PEPTIDE TRANSPORTER family members in plants. *Trends Plant Sci.* 19:5–9
66. Li F, Ma C, Wang X, Gao C, Zhang J, et al. 2011. Characterization of *Sucrose transporter* alleles and their association with seed yield-related traits in *Brassica napus* L. *BMC Plant Biol.* 11:168
67. Liao M, Cao E, Julius D, Cheng Y. 2013. Structure of the TRPV1 ion channel determined by electron cryo-microscopy. *Nature* 504:107–12
68. Lu P, Bai XC, Ma D, Xie T, Yan C, et al. 2014. Three-dimensional structure of human γ-secretase. *Nature* 512:166–70
69. Madej MG, Sun L, Yan N, Kaback HR. 2014. Functional architecture of MFS D-glucose transporters. *PNAS* 111:E719–27
70. Maiden MC, Davis EO, Baldwin SA, Moore DC, Henderson PJ. 1987. Mammalian and bacterial sugar transport proteins are homologous. *Nature* 325:641–43
71. Marger MD, Saier MH Jr. 1993. A major superfamily of transmembrane facilitators that catalyse uniport, symport and antiport. *Trends Biochem. Sci.* 18:13–20
72. Meyerson JR, Kumar J, Chittori S, Rao P, Pierson J, et al. 2014. Structural mechanism of glutamate receptor activation and desensitization. *Nature* 514:328–34
73. Mueckler M, Caruso C, Baldwin SA, Panico M, Blench I, et al. 1985. Sequence and structure of a human glucose transporter. *Science* 229:941–45
74. Mueckler M, Thorens B. 2013. The SLC2 (GLUT) family of membrane transporters. *Mol. Asp. Med.* 34:121–38
75. Murata K, Mitsuoka K, Hirai T, Walz T, Agre P, et al. 2000. Structural determinants of water permeation through aquaporin-1. *Nature* 407:599–605
76. Newstead S. 2014. Molecular insights into proton coupled peptide transport in the PTR family of oligopeptide transporters. *Biochim. Biophys. Acta* 1850:488–99
77. Newstead S, Drew D, Cameron AD, Postis VL, Xia X, et al. 2011. Crystal structure of a prokaryotic homologue of the mammalian oligopeptide–proton symporters, PepT1 and PepT2. *EMBO J.* 30:417–26
78. Nguyen LN, Ma D, Shui G, Wong P, Cazenave-Gassiot A, et al. 2014. Mfsd2a is a transporter for the essential omega-3 fatty acid docosahexaenoic acid. *Nature* 509:503–6
79. Oka Y, Asano T, Shibasaki Y, Lin J-L, Tsukuda K, et al. 1990. C-terminal truncated glucose transporter is locked into an inward-facing form without transport activity. *Nature* 345:550–53
80. Oldham ML, Chen J. 2011. Crystal structure of the maltose transporter in a pretranslocation intermediate state. *Science* 332:1202–5
81. Özcan S, Johnston M. 1999. Function and regulation of yeast hexose transporters. *Microbiol. Mol. Biol. Rev.* 63:554–69
82. Parker JL, Newstead S. 2014. Molecular basis of nitrate uptake by the plant nitrate transporter NRT1.1. *Nature* 507:68–72
83. Pedersen BP, Kumar H, Waight AB, Risenmay AJ, Roe-Zurz Z, et al. 2013. Crystal structure of a eukaryotic phosphate transporter. *Nature* 496:533–36
84. Quistgaard EM, Löw C, Moberg P, Trésaugues L, Nordlund P. 2013. Structural basis for substrate transport in the GLUT-homology family of monosaccharide transporters. *Nat. Struct. Mol. Biol.* 20:766–68

85. Rask-Andersen M, Masuram S, Fredriksson R, Schiöth HB. 2013. Solute carriers as drug targets: current use, clinical trials and prospective. *Mol. Asp. Med.* 34:702–10
86. Rasmussen SGF, Choi H-J, Fung JJ, Pardon E, Casarosa P, et al. 2011. Structure of a nanobody-stabilized active state of the β_2 adrenoceptor. *Nature* 469:175–80
87. Reimer RJ. 2013. SLC17: a functionally diverse family of organic anion transporters. *Mol. Asp. Med.* 34:350–59
88. Reyes N, Ginter C, Boudker O. 2009. Transport mechanism of a bacterial homologue of glutamate transporters. *Nature* 462:880–85
89. Robertson DE, Kaczorowski GJ, Garcia ML, Kaback HR. 1980. Active transport in membrane vesicles from *Escherichia coli*: The electrochemical proton gradient alters the distribution of the *lac* carrier between two different kinetic states. *Biochemistry* 19:5692–702
90. Saier MH Jr, Reddy VS, Tamang DG, Västermark Å. 2014. The transporter classification database. *Nucleic Acids Res.* 42:D251–58
91. Sanderson NM, Qi D, Steel A, Henderson PJF. 1998. Effect of the $D^{32}N$ and $N^{300}F$ mutations on the activity of the bacterial sugar transport protein, GalP. *Biochem. Soc. Trans.* 26:S306
92. Schürmann A, Doege H, Ohnimus H, Monser V, Buchs A, Joost H-G. 1997. Role of conserved arginine and glutamate residues on the cytosolic surface of glucose transporters for transporter function. *Biochemistry* 36:12897–902
93. Shi Y. 2013. Common folds and transport mechanisms of secondary active transporters. *Annu. Rev. Biophys.* 42:51–72
94. Shuman HA. 1981. The use of gene fusions of study bacterial transport proteins. *J. Membr. Biol.* 61:1–11
95. Skou JC. 1957. The influence of some cations on an adenosine triphosphatase from peripheral nerves. *Biochim. Biophys. Acta* 23:394–401
96. Smith DE, Clémençon B, Hediger MA. 2013. Proton-coupled oligopeptide transporter family SLC15: physiological, pharmacological and pathological implications. *Mol. Asp. Med.* 34:323–36
97. Solcan N, Kwok J, Fowler PW, Cameron AD, Drew D, et al. 2012. Alternating access mechanism in the POT family of oligopeptide transporters. *EMBO J.* 31:3411–21
98. Steyaert J, Kobilka BK. 2011. Nanobody stabilization of G protein-coupled receptor conformational states. *Curr. Opin. Struct. Biol.* 21:567–72
99. Sun J, Bankston JR, Payandeh J, Hinds TR, Zagotta WN, Zheng N. 2014. Crystal structure of the plant dual-affinity nitrate transporter NRT1.1. *Nature* 507:73–77
100. Sun L, Zeng X, Yan C, Sun X, Gong X, et al. 2012. Crystal structure of a bacterial homologue of glucose transporters GLUT1–4. *Nature* 490:361–66
101. Thorens B, Mueckler M. 2010. Glucose transporters in the 21st century. *Am. J. Physiol. Endocrinol. Metab.* 298:E141–45
102. Thorens B, Sarkar HK, Kaback HR, Lodish HF. 1988. Cloning and functional expression in bacteria of a novel glucose transporter present in liver, intestine, kidney, and β-pancreatic islet cells. *Cell* 55:281–90
103. Vitavska O, Wieczorek H. 2013. The SLC45 gene family of putative sugar transporters. *Mol. Asp. Med.* 34:655–60
104. Wang T, Fu G, Pan X, Wu J, Gong X, et al. 2013. Structure of a bacterial energy-coupling factor transporter. *Nature* 497:272–76
105. Wang Y, Huang Y, Wang J, Cheng C, Huang W, et al. 2009. Structure of the formate transporter FocA reveals a pentameric aquaporin-like channel. *Nature* 462:467–72
106. Widdas WF. 1951. Inability of diffusion to account for placental glucose transfer in the sheep. *J. Physiol.* 115:36–37
107. Widdas WF. 1952. Inability of diffusion to account for placental glucose transfer in the sheep and consideration of the kinetics of a possible carrier transfer. *J. Physiol.* 118:23–39
108. Wilbrandt W, Guensberg E, Lauener H. 1947. Admission of glucose by erythrocyte membrane. *Helv. Physiol. Pharmacol. Acta* 5:C20–22
109. Wilson-O'Brien AL, Patron N, Rogers S. 2010. Evolutionary ancestry and novel functions of the mammalian glucose transporter (GLUT) family. *BMC Evol. Biol.* 10:152
110. Wisedchaisri G, Park M-S, Iadanza MG, Zheng H, Gonen T. 2014. Proton-coupled sugar transport in the prototypical major facilitator superfamily protein XylE. *Nat. Commun.* 5:4521

111. Wong FH, Chen JS, Reddy V, Day JL, Shlykov MA, et al. 2012. The amino acid-polyamine-organocation superfamily. *J. Mol. Microbiol. Biotechnol.* 22:105–13
112. Xu K, Zhang M, Zhao Q, Yu F, Guo H, et al. 2013. Crystal structure of a folate energy-coupling factor transporter from *Lactobacillus brevis*. *Nature* 497:268–71
113. Yamashita A, Singh SK, Kawate T, Jin Y, Gouaux E. 2005. Crystal structure of a bacterial homologue of Na^+/Cl^--dependent neurotransmitter transporters. *Nature* 437:215–23
114. Yan H, Huang W, Yan C, Gong X, Jiang S, et al. 2013. Structure and mechanism of a nitrate transporter. *Cell Rep.* 3:716–23
115. Yan N. 2013. Structural advances for the major facilitator superfamily (MFS) transporters. *Trends Biochem. Sci.* 38:151–59
116. Yan N. 2013. Structural investigation of the proton-coupled secondary transporters. *Curr. Opin. Struct. Biol.* 23:483–91
117. Yin Y, He X, Szewczyk P, Nguyen T, Chang G. 2006. Structure of the multidrug transporter EmrD from *Escherichia coli*. *Science* 312:741–44
118. Young JD, Yao SYM, Baldwin JM, Cass CE, Baldwin SA. 2013. The human concentrative and equilibrative nucleoside transporter families, SLC28 and SLC29. *Mol. Asp. Med.* 34:529–47
119. Zhang P, Wang J, Shi Y. 2010. Structure and mechanism of the S component of a bacterial ECF transporter. *Nature* 468:717–20
120. Zhao R, Goldman ID. 2013. Folate and thiamine transporters mediated by facilitative carriers (SLC19A1-3 and SLC46A1) and folate receptors. *Mol. Asp. Med.* 34:373–85
121. Zhao Y, Mao G, Liu M, Zhang L, Wang X, Zhang XC. 2014. Crystal structure of the *E. coli* peptide transporter YbgH. *Structure* 22:1152–60
122. Zheng H, Wisedchaisri G, Gonen T. 2013. Crystal structure of a nitrate/nitrite exchanger. *Nature* 497:647–51
123. Zhou X, Levin EJ, Pan Y, McCoy JG, Sharma R, et al. 2014. Structural basis of the alternating-access mechanism in a bile acid transporter. *Nature* 505:569–73
124. Zhou Y, Jiang X, Kaback HR. 2012 . Role of the irreplaceable residues in the LacY alternating access mechanism. *PNAS* 109:12438–42

RELATED RESOURCES

Genomic Transporter Database, SLC series (the SLC Tables): **http://slc.bioparadigms.org/**
Membrane proteins of known structures: **http://blanco.biomol.uci.edu/mpstruc/**
The MFS Clan (CL0015) in the Pfam protein families database: **http://pfam.xfam.org/clan/MFS**
Transporter Classification Database: **http://www.tcdb.org/**